Kocatepe Veterinary Journal

Kocatepe Vet J. (2024):17(2):104-116

DOI: 10.30607/kvj.1430771

RESEARCH ARTICLE

Novel Thiazole/Ethyl Thiazole Carboxylate-Acetamide Derivatives and Their Cytotoxic Effect Evaluation

Asaf Evrim EVREN[1,2,3*], Sam DAWBA[2,4,5], Demokrat NUHA[2,6], Aybüke Züleyha KAYA[2], Zerrin CANTÜRK[7], Leyla YURTTAŞ[2]

[1]Department of Pharmacy Services, Vocational School of Health Services, Bilecik Şeyh Edebali University, Bilecik, Türkiye
[2]Department of Pharmaceutical Chemistry, Faculty of Pharmacy, Anadolu University, Eskişehir, Türkiye
[3]Department of Analytical Chemistry, Faculty of Pharmacy, Anadolu University, Eskişehir, Türkiye
[4]Department of Doctor of Pharmacy (PharmD), Faculty of Medical Sciences, Thamar University, Dhamar, Yemen
[5]Department of Pharmacy, Faculty of Medical Sciences, Al-Hikma University, Dhamar, Yemen
[6]Department of Doctor of Science in Chemistry, Faculty of Pharmacy, University for Business and Technology, Prishtina, Kosovo
[7]Department of Pharmaceutical Microbiology, Faculty of Pharmacy, Anadolu University, Eskişehir, Türkiye

ABSTRACT

In this study, the main goal is to determine the anticancer compound(s) that can be used against A549 non-small lung epithelial carcinoma, Caco-2 colon carcinoma, and SHSY-5Y neuroblastoma cells with high selectivity. For this purpose, our study group synthesized two similar acetamide series: four compounds (3a–3d), including thiazole, and four compounds (3e–3h), including ethyl (4-methyl-thiazol-5-yl)carboxylate. The structural analyses of eight compounds were identified by HRMS, ^{1}H-NMR, and ^{13}C-NMR. After approving the purity, their anticancer profiles were evaluated against above cancer cells, and the cytotoxicity effect was also tested against NIH/3T3 fibroblast cells. Meanwhile, ADME and DFT calculations indicated that compounds have good ADME profiles and chemical stability. Among the targeted compounds, compound 3g exhibits greater stability. In chemical systems, stability is important because it represents the energy balance within a molecule. The results showed that compounds have significant impact on SHSY-5Y cells with higher selectivity than other cells. The combination of ester groups on thiazole and thiazoline (compound 3g) was found to be significantly more effective than doxorubicin and highly selective on SHSY-5Y cells than healthy cells. Besides that, combination of thiazole and triazole (3d and 3h) decreased antiproliferative activity in three cancer cells while increasing cytotoxicity in healthy cells. This study suggests that future perspectives in studies regarding the treatments of neuroblastoma and its related diseases of ethyl 2-acetamido-4-methylthiazole-5-carboxylate and thiazoline combination are encouraging.

Keywords: Anticancer activity, DFT, Ethyl carboxylate, SHSY-5Y, Thiazole

***

Yeni Tiyazol/Etil Tiyazol Karboksilat-Asetamid Türevleri ve Bunların Sitotoksik Etkisinin Değerlendirilmesi

ÖZ

Bu çalışmada A549 küçük olmayan akciğer epitelyal karsinomu, Caco-2 kolon karsinomu ve SHSY-5Y nöroblastoma hücrelerine karşı kullanılabilecek yüksek seçiciliğe sahip antikanser bileşik(ler)in belirlenmesi temel amaçtır. Bu amaçla çalışma grubumuz tarafından tiyazol içeren dört bileşik (**3a-3d**) ve etil (4-metil-tiyazol-5-il)karboksilat içeren dört bileşik (**3e-3h**) şeklinde benzer iki asetamit serisi sentezlendi. Bu sekiz bileşiğin yapısal analizleri HRMS, ^{1}H-NMR ve ^{13}C-NMR yöntemleri ile gerçekleştirildi. Bileşiklerin saf bir şekilde elde edildikleri tespit edildikten sonra bahsedilen kanser hücrelerine karşı antikanser profilleri değerlendirildi ve ayrıca NIH/3T3 fibroblast hücrelerine karşı sitotoksik etkisi incelendi. Aynı zamanda ADME ve DFT hesaplamaları sonucunda bileşiklerin iyi ADME profiline ve kimyasal stabiliteye sahip olduğu belirlendi. Hedeflenen bileşikler arasında bileşik **3g** daha fazla stabilite sergilemektedir. Kimyasal sistemlerde stabilite önemlidir çünkü bir molekül içindeki enerji dengesini temsil eder. Sonuçlar, bileşiklerin SHSY-5Y hücreleri üzerinde diğer hücrelere göre daha seçici bir etkiye sahip olduğunu gösterdi. Tiyazol üzerindeki ester grubu ile tiyazolidin (bileşik **3g**) kombinasyonunun doksorubisinden anlamlı derecede etkili olduğu ve SHSY-5Y hücreleri üzerinde sağlıklı hücrelere göre oldukça seçici olduğu bulundu. Bunun yanı sıra, tiyazol-triazol kombinasyonu (**3d** ve **3h**) üç kanser hücresinde de antiproliferatif aktiviteyi azaltırken, sağlıklı hücrede sitotoksisiteyi arttırdı. Bu çalışma ile nöroblastoma ve bununla ilişkili hastalıkların tedavisine ilişkin çalışmalarda etil 2-asetamido-4-metiltiyazol-5-karboksilat ve tiyazolin kombinasyonunun ileride gerçekleştirilecek çalışmalar için ümit verici olduğunu ileri sürmektedir.

Anahtar Kelimeler: Antikanser aktivite, DFT, Etil karboksilat, SHSY-5Y, Tiyazol

To cite this article: Evren A.E. Dawba S. Nuha D. Kaya A.Z. Cantürk Z. Yurttaş L. Novel Thiazole/Ethyl Thiazole Carboxylate-Acetamide Derivatives and Their Cytotoxic Effect Evaluation. Kocatepe Vet J. (2024):17(2):104-116

Submission: 03.02.2024 **Accepted**: 28.05.2024 **Published Online**: 07.06.2024

ORCID ID; *AEE: 0000-0002-8651-826X, SD: 0000-0001-7001-0739, DN: 0000-0002-7271-6791, AZK: 0009-0002-1614-2380, ZC: 0000-0001-7709-4285, LY: 0000-0002-0957-6044*

*Corresponding author e-mail: asafevrimevren@gmail.com

INTRODUCTION

Cancer is a general term used to describe a number of diseases that are caused by the uncontrolled division of cells. (Hernandes et al. 2023). Regardless of the type of cancer, necrotic death of cancer cells is one of the main problems (Ocansey et al. 2024; Sharifi et al. 2019). Even worse, it does not affect only humankind but also affects animals. Human and animal cancer mortality rates show that the most common cause of death is (Oh & Cho 2023a; Sarver et al. 2022). Moreover, in decades, the researchers explored the similarity between the prognosis of cancer in humans and animals (Cavalier et al. 2023; Cortes 2019), as well as the helpful and unhelpful aspects of having a companion animal for people with cancer who are dealing with the emotional challenges that come with diagnosis and treatment. (McGhee et al. 2022; Nitkin 2014; Nitkin & Buchanan 2020). Although these reports were tested on a small-scale population part by part, they all indicated very similar results. The pathophysiological development of cancer in humans and animals is very similar, and the treatment of cancer in both species together has a positive impact on treatment. This means that the treatment options can be applied to both humans and their pets (Oh & Cho 2023b; Pinho et al. 2012).

Approaches in cancer treatments vary widely, especially radiotherapy (Delaney et al. 2005; Freitas et al. 2023), chemotherapy (Falzone et al. 2023; Xing et al. 2024; Yang et al. 2023), and biomarkers (Dora et al. 2023; Tarighati et al. 2023) are promising in many ways. In the last two decades, there have been valuable improvements after the approval of some small-molecule inhibitors (Gallego & Varani 2001; Hoelder et al. 2012; Roskoski Jr 2024; Wu et al. 2015). Unfortunately, the incidence of cancer is increasing day by day and, in many cases, the misdiagnosis or the incorrect application of the treatment can worsen the condition of the patient. (Kavitha et al. 2022; Kwon et al. 2015). For this reason, the protocols for the treatment of cancer should be reorganized and improved. Besides, the experience clinically in the past points out that the other real problem in the future will be useless because of developing resistance against current drugs (Eslami et al. 2024; Holohan et al. 2013; Housman et al. 2014; Li et al. 2024; Tolomeo & Simoni 2002). Because of that, cancer studies must go on immediately in every aspect. For example, designing and synthesizing new chemotherapeutics seems like a useful option to address this issue (Laiolo et al. 2024; Xiong et al. 2024). Since we perpetually need a new agent that has a selective anticancer effect, in this study, we designed and synthesized novel nitrogen-containing heterocyclic molecules to test their antitumoral activity. The main core was formed with two different thiazole rings, and their derivatives were designed with imidazole, triazole, tetrazole, and thiazoline rings linked with an acetamide bridge. Here, one of the main purposes is to discuss the effect of the ester group of thiazole, and the second is to determine the anticancer activity ability of the heterocycles. We chose these varieties because the cytotoxic activity of thiazole (Evren et al. 2023; Özkay et al. 2022), imidazole (Osmaniye et al. 2022), triazole (Saffour et al. 2024), tetrazole (Dileep et al. 2017) and thiazoline (Altintop et al. 2014) was previously reported against various cancer cells. Additionally, the drugs approved for anticancer treatments, as shown in Figure 1, include these ring systems.

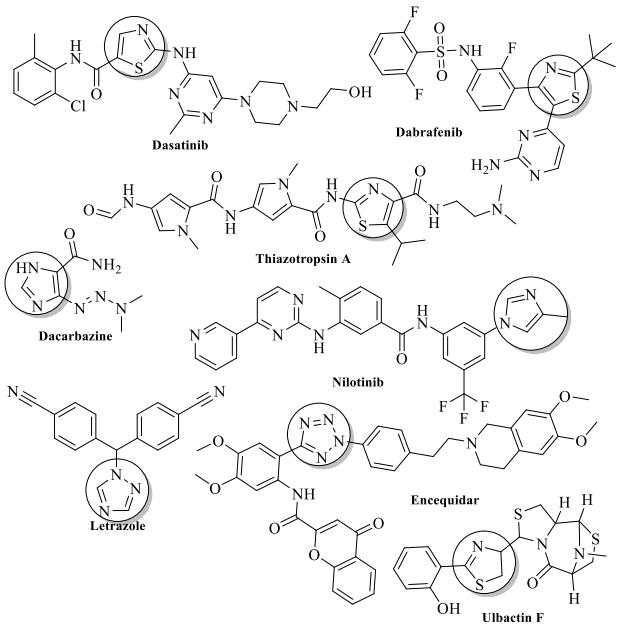

Figure 1: Some anticancer drugs and their ring systems.

In addition to the above, thiazole ring was reported many times because of its anticancer properties against A549, Caco-2, and SH-SY5Y cell lines. Against A549 cells, when this ring system was especially linked with amide bridge (Evren et al. 2019a; Evren et al. 2019b) showed valuable cytotoxicity effects. On the other hand, according to the literature (Bhagat et al. 2021; Catarzi et al. 2022; El-Gazzar et al. 2017; Singh et al. 2022), thioether group linked to thiazole positively affected anti-neuroblastoma and anti-colon adenocarcinoma activities. Also, the thiazole ring system is favorable in anticancer drug development due to inducing apoptosis properties by medicinal chemists (Ahmed et al. 2009; Bhat et al. 2009; Wang et al. 2024; Xiong et al. 2019). All these properties inspired us to develop new anticancer molecules using thiazole core combined with thioether and amide bridges. Therefore, it was portended that using this combination will successfully result in reaching novel and effective anticancer agents.

Given the foregoing details, two related series (thiazole-acetamide and novel ethyl thiazole carboxylate-acetamide analogs) were generated and synthesized for this study, after which their cytotoxicity and physicochemical profiles were examined. Finally, the structure-activity relationship (SAR) was reported.

MATERIALS AND METHODS

Chemistry

All chemicals used in the syntheses were purchased either from Merck Chemicals (Merck KGaA, Darmstadt, Germany) or Sigma-Aldrich Chemicals (Sigma-Aldrich Corp., St. Louis, MO, USA). The compounds were monitored for reactions and purities using thin-layer chromatography (TLC) with silica gel 60 F254 aluminum sheets that were purchased from Merck (Darmstadt, Germany). The MP90 digital melting point apparatus (Mettler Toledo, Ohio, USA) was used to record the melting points of the synthesized compounds, and the results were given without correction. ^{1}H NMR and ^{13}C NMR spectra were recorded by a Bruker 300 MHz and 75 MHz digital FT-NMR spectrometer (Bruker Bioscience, Billerica, MA, USA) in DMSO-d_6, respectively. Splitting patterns in the NMR spectra were denoted by the following symbols: s for singlet, d for doublet, t for triplet, and m for multiplet. Coupling constants (J) were reported as Hertz. High-resolution mass spectrometric (HRMS) analyses were performed using an LC/MS-IT-TOF system (Shimadzu, Kyoto, Japan). Elemental analyses were performed on a Leco 932 CHNS analyzer (Leco, Michigan, USA). The whole synthesis plan is illustrated in Scheme 1.

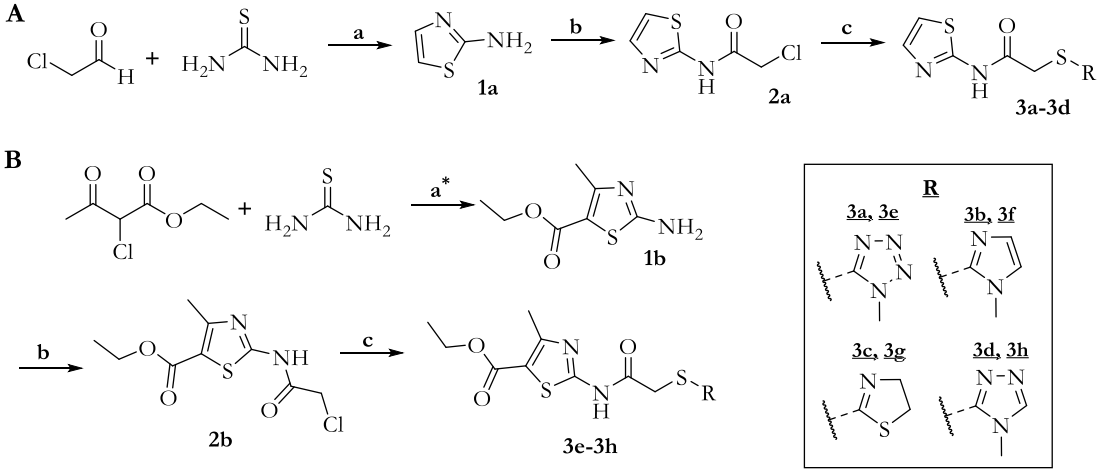

Scheme 1. Synthesis plan. A: Stepwise synthesis of compounds 3a-3d, B: Stepwise synthesis of compounds 3e-3h; a: EtOH, reflux 4 hrs; **a*:** THF, 0°C/rt 30 min/reflux 8 hrs; **b:** 2-chloroacetyl chloride, THF, TEA, 0°C, **c:** Mercaptoheterocycles, Me_2CO, K_2CO_3, rt. 2 hrs.

Synthesis of 2-aminothiazole and ethyl 2-amino-5-methylthiazole-4-carboxylate (1a, 1b)

Chloro acetaldehyde (40.76 mmol, 2.59 ml) was mixed with ethanol and added slowly into a flask containing an equivalent amount of thiourea (40.76 mmol, 3.103 g) in ethanol while in an ice bath. The mixture was stirred at room temperature for 4 hours. The mixture was then poured into ice-cold water. The resulting precipitate was filtered and, after drying, recrystallized in ethanol.

Ethyl 2-chloroacetoacetate (18.84 mmol, 2.61 ml) was added dropwise into a flask containing thiourea (18.84 mmol, 1.434 g) dissolved in tetrahydrofuran in a cold environment controlled using an ice bath. After the addition of the acetate derivative, the mixture was stirred for 30 minutes in the same conditions, then refluxed for 8 hours. Following the end of the reaction, the solvent was evaporated, and the residue was recrystallized from ethanol.

Synthesis of 2-chloro-N-(thiazol-2-yl)acetamide (2a) / ethyl 2-(2-chloroacetamido)-5-methylthiazole-4-carboxylate (2b)

To the previously obtained compound 1a/1b dissolved in tetrahydrofuran (THF), triethyl amine (TEA) (1: 3 eq.) was added, followed by the dropwise addition of 2-chloroacetyl chloride (1: 1 eq.), while the reaction conditions were controlled by an ice bath. The mixture was stirred for another hour after the addition. After determining the end of the reaction using TLC, THF was evaporated, and the remaining residue was washed using water and filtered. The final residue was recrystallized from ethanol.

Synthesis of 2-chloro-N-(thiazol-2-yl) acetamide derivatives (3a-3d) and ethyl 2-(2-chloroacetamido)-5-methylthiazole-4-carboxylate (3e-3h)

Compound 2a/2b was added to a solution of the appropriate mercapto derivative (1 eq.) and potassium carbonate (1.5 eq.) in acetone. 1-Methyl-1H-tetrazole-5-thiol, 1-methyl-1H-imidazole-2-thiol, 4,5-dihydrothiazole-2-thiol, and 4-methyl-4H-1,2,4-triazole-3-thiol were the mercapto derivatives used in the synthesis, as illustrated in Scheme 1. The mixture was stirred at room temperature for 2 minutes, and its completeness was checked using TLC. Following the evaporation of the solvent, the residue was cleaned and collected through filtration. The final residue was recrystallized from ethanol.

Ethyl 5-methyl-2-[2-((1-methyl-1H-tetrazol-5-yl) thio)acetamido]thiazole-4-carboxylate (3e)

m. p. 206-207 °C, ^{1}H NMR (300 MHz) (DMSO-d_6) δ (ppm): 1.27 (t, J= 7.08 Hz, 3H, aliphatic CH_3), 2.54 (s, 3H, thiazole- CH_3), 3.98 (s, 3H, tetrazole- CH_3), 4.22 (q, J= 7.10 Hz, 2H, aliphatic CH_2), 4.34 (s, 2H, CO-CH_2-S), 12.85 (brs, H, N-H). ^{13}C NMR (75 MHz) (DMSO-d_6) δ (ppm): 14.67 (thiazole- CH_3), 17.52 (aliphatic- CH_3), 34.14 (tetrazole- CH_3), 37.20 (CO-CH_2-S), 60.88 (COO-CH_2-), 114.24 (thiazole C-5), 153.64 (thiazole C-4), 156.76 (tetrazole C-5), 161.03 (thiazole C-2), 162.57 (carboxyl), 167.50 (carbonyl). For $C_{11}H_{14}N_6O_3S_2$ calculated: Elem. Anal.: C, 38.59%; H, 4.12%; N, 24.54%; O, 14.02%; S, 18.73%, found: C, 38.56%; H, 4.11%; N, 24.57%; O, 14.02; S, 18.74%. HRMS (m/z): $[M + 1]^+$ calculated 343.0642; found 343.0642.

Ethyl 5-methyl-2-[2-((1-methyl-1H-imidazol-2-yl)thio)acetamido]thiazole-4-carboxylate (3f)

m. p. 275-276 °C, ^{1}H NMR (300 MHz) (DMSO-d_6) *δ* (ppm): 1.27 (t, *J*= 7.09 Hz, 3H, aliphatic CH_3), 2.54 (s, 3H, thiazole- CH_3), 3.59 (s, 3H, imidazole- CH_3), 3.97 (s, 2H, CO-CH_2-S), 4.23 (q, *J*= 7.09 Hz, 2H, aliphatic CH_2), 6.94 (d, *J*= 1.09 Hz, H, imidazole-H), 7.26 (d, *J*= 1.01 Hz, H, imidazole-H), 12.83 (brs, H, N-H). ^{13}C NMR (75 MHz) (DMSO-d_6) *δ* (ppm): 14.65 (thiazole-CH_3), 17.48 (aliphatic- CH_3), 33.46 (imidazole- CH_3), 37.38 (CO-CH_2-S), 61.01 (COO-CH_2-), 114.67 (thiazole C-5), 124.19 (imidazole C-5), 129.12 (imidazole C-4), 135.10 (imidazole C-2), 156.72 (thiazole C-4), 159.80 (thiazole C-2), 162.50 (carboxyl), 168.35 (carbonyl). For $C_{13}H_{16}N_4O_3S_2$ calculated: Elem. Anal.: C, 45.87%; H, 4.74%; N, 16.46%; O, 14.10%; S, 18.84%, found: C, 45.85%; H, 4.71%; N, 16.43%; O, 14.12%; S, 18.86%. HRMS (m/z): $[M + 1]^+$ calculated 341.0737; found 341.0744.

Ethyl 2-[2-((4,5-dihydrothiazol-2-yl)thio)acetamido]-5-methylthiazole-4-carboxylate (3g)

m. p. 275-276 °C, ^{1}H NMR (300 MHz) (DMSO-d_6) *δ* (ppm): 1.27 (t, *J*= 7.09 Hz, 3H, aliphatic CH_3), 2.54 (s, 3H, thiazole-CH_3), 3.47 (t, *J*= 7.99 Hz, 2H, dihydrothiazole-H), 4.09 (t, *J*= 7.99 Hz, 2H, dihydrothiazole-H), 4.18 (s, 2H, CO-CH_2-S) 4.24 (q, *J*= 7.09 Hz, 2H, aliphatic-CH_2), 12.70 (brs, H, N-H). ^{13}C NMR (75 MHz) (DMSO-d_6) *δ* (ppm): 14.65 (thiazole-CH_3), 17.47 (aliphatic-CH_3), 36.04 (CO-CH_2-S), 36.20 (dihydrothiazole C-5), 61.00 (COO-CH_2-), 64.35 (dihydrothiazole C-4) 114.67 (thiazole C-5), 156.68 (thiazole C-4), 159.84 (thiazole C-2), 162.49 (dihydrothiazole C-2), 162.86 (carboxyl), 167.35 (carbonyl). For $C_{12}H_{15}N_3O_3S_3$ calculated: Elem. Anal.: C, 41.72%; H, 4.38%; N, 12.16%; O, 13.89%; S, 27.85%, found: C, 41.75%; H, 4.36%; N, 12.14%; O, 13.89; S, 27.86%. HRMS (m/z): $[M + 1]^+$ calculated 346.0348; found 346.0352.

Chemical Theoretical Calculations

Theoretical approaches for 2-mercapto-*N*-(thiazol-2-yl)acetamide derivatives (3a-3h) were run using the molecular visualization programs Gaussian 09 W (Frisch et al. 2009) and GaussView 5.0 (Dennington et al. 2009). Density Functional Theory (DFT) calculations were done according to previous studies (Nuha et al. 2022; Nuha et al. 2023). Total electric dipole moment (μ_{tot}) calculated theoretically by using the following equations: (Hernández-Paredes et al. 2009; Kleinman 1962).

$$\mu_{tot} = (\mu_x^2 + \mu_y^2 + \mu_z^2)^{1/2} (1)$$

ADME calculation

The physicochemical descriptors of the final compounds were computed using SwissADME software. Molecular weight (MW), H-bond acceptors number (NHA), H-bond donors number (NHD), topological polar surface area (TPSA), partition coefficient (Log P), and gastrointestinal absorption properties (GI abs) were calculated for compounds 3a–3h.

Biological Activities

Cell line and Cell culture

A549 human lung adenocarcinoma cells (ATCC number CCL-185™), Caco-2 Human Colorectal Adenocarcinoma cells (ATCC number HTB-37™), SH-SY5Y human neuroblastoma cells (ATCC number CRL-2266™) and NIH3T3 mouse healthy fibroblast cells (ATCC number CRL-1658™) were obtained from the American Type Culture Collection. All cells were grown and prepared as descripted in previous studies (Dawbaa et al. 2023; Yurttas et al. 2024; Yurttaş et al. 2023). The control group (solvent control) was prepared with a medium containing 0.1% DMSO. Doxorubicin used as a positive control.

MTT Cytotoxicity assay

The synthesized compounds (3a–3h) were tested for their cytotoxicity in vitro, in comparison with doxorubicin as a reference drug, against A549, Caco-2, SH-SY5Y, and NIH3T3 cells. This method was applied as in previous studies (Dawbaa et al. 2021; Yurttaş et al. 2020; Yurttaş et al. 2019).

RESULTS

Chemistry

The complete synthetic plan of eight targeted compounds (3a–3h) is illustrated in Scheme 1. To synthesize these products, they were divided into two groups as the starting reactants were different. Synthesis of compounds 3a-3d group started with reacting 2-chloroacetaldehyde with equivalent amount of thiourea to produce 2-aminothiazole, which was acetylated with 2-chloroacetyl chloride, and finally the resulting 2-chloro-*N*-(thiazol-2-yl)acetamide was reacted with four different thiol derivatives to produce compounds 3a-3d. The second group, 3e-3h, was synthesized starting with the reaction of ethyl-2-chloroacetoacetate with thiourea. The resulting 2-amino-5-methylthiazole-4-carboxylate was also acetylated using 2-chloroacetychloride, which then reacted with thiol derivatives to produce compounds 3e–3h. Structure elucidation was achieved by ^{1}H-NMR, ^{13}C-NMR, elemental analysis, and High-Resolution Mass Spectrometry (HRMS). The peaks in ^{1}H-NMR and ^{13}C-NMR spectra were observed in the predicted chemical shifts. Elemental analysis and mass peaks [M+1] of the compounds agreed with the predicted molecular formulae.

The ^{1}H-NMR spectra showed singlet peaks at δ 3.98 ppm for methyl hydrogens of tetrazole, while those at 3.59 ppm are for methyl hydrogens of imidazole and triazole. The singlet peak occurring at 2.53-2.54 ppm is for the 5-methyl hydrogens of thiazole. The methylene group bridging the carbonyl with the sulphur atom kept showing between 3.97-4.36 ppm as a singlet. Hydrogen peaks of methylenes numbers 5 and 4 of 4,5-dihydrothiazole belonging to compound 3c are shown as triplets at 3.47 ppm and 4.10 ppm, respectively. In the aromatic region, hydrogens at carbons 5 and 4 of thiazole of compounds 3a–3d kept showing as doublets at around 7.23 ppm and 7.47 ppm, respectively. Hydrogens on carbons 4 and 5 of imidazole in compounds 3b and 3f have doublets at around 6.95 ppm and 7.26 ppm, respectively. A singlet at 8.55 ppm confirms that compound 3d and compound 3h contain only one hydrogen of triazole. The amidic hydrogen present in all synthesized molecules is shown as a broad singlet above 12 ppm.

^{13}C-NMR spectra confirmed the ^{1}H-NMR results. The carbon of methyl groups appeared in slightly different shifts according to their position in the molecule. Signals at 34.18, 33.45, and 31.29 ppm were observed to represent the carbon of the methyl group in tetrazole, imidazole, and triazole, respectively. The methyl group carbon in thiazole of compounds 3a-3d showed signals at around 14.65 ppm. The methylene bridge between carbonyl and sulphur showed signals in the range 36-37.5 ppm. The terminal methyl group carbon in the ester of compounds 3e-3h was observed in negligibly different shifts in the range 17.47-17.55 ppm. Similarly, the methylene carbon of the ester kept showing at 60.83-61.01 ppm. The aromatic region in the range of 100-170 ppm showed different signals representing different carbons in the aromatic rings. These carbons were assigned individually in the ^{13}C-NMR analytical monographs below. The carbonyl carbons have shown signals in the range 165.88-168.35 ppm, whereas the signals of the carboxylic carbon of compounds 3e-3h were observed in 161.30-162.86 ppm.

For every targeted compound, the elemental analyses of C, H, and N yielded results that were in line with Mass analyses. It also revealed that the M+1 peaks identified by LC-MS/MS validated the structures of the corresponding molecules and matched their calculated values.

Prediction of physicochemical properties

The pharmacokinetic properties of final compounds were predicted using Swiss ADME and the calculated values were represented in Table 1.

Table 1. Some physicochemical properties of the compounds **(3a-3h)**

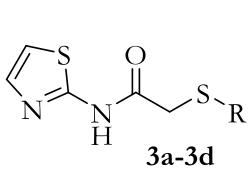

3a-3d

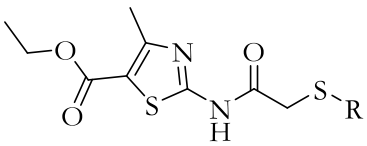

3e-3h

Compounds	R	MW	NHA	NHD	TPSA (A°)	Log P	GI abs
3a	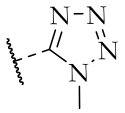	256.31	5	1	139.13	0.57	High
3b	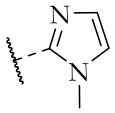	254.33	3	1	113.35	1.10	High
3c	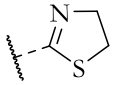	259.37	3	1	133.19	1.43	High
3d	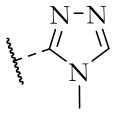	255.32	4	1	126.24	0.71	High
3e	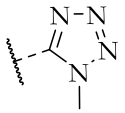	342.40	7	1	165.43	1.30	Low
3f	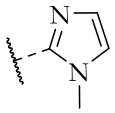	340.42	5	1	139.65	1.82	High
3g	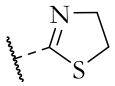	345.46	5	1	159.49	2.17	Low
3h	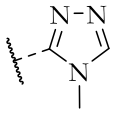	341.41	6	1	152.54	1.44	Low

MW: Molecular weight, **NHA:** No H-bond acceptors, **NHD:** No H-bond donors, **TPSA:** Topological polar surface area, **Log P:** Partition coefficient, **GI abs:** Gastrointestinal absorption

Molecular weight (MW), number of H-bond acceptors (NHA), number of H-bond donors (NHD), topological polar surface area (TPSA), partition coefficient (Log P), and gastrointestinal absorption properties (GI abs) are some of the important parameters for determining the absorption, distribution, metabolism, and excretion (ADME) processes of a drug in the process leading to a biological response in an organism. According to calculations, compounds 3a–3h possess a molecular weight between 256.31-345.46 g/mol, hydrogen bond acceptor bonds between 3-7 and one hydrogen donor bond. It was seen that there were two more hydrogen acceptors in 3e-3h compounds compared to corresponding 3a-3d compounds due to -COOEt function. The TPSA of the compounds was predicted between 113.35-165.43 Å, whereas log P was calculated between 0.57-2.17. These findings were appropriate to Lipinski rule of five for oral drug probability. Gastrointestinal absorption was predicted as high except three compounds 3e, 3g and 3h.

Theoretical calculations

Using DFT/ B3LYP/6-31G(d,p), optimized molecular structures with total energy values of 2-mercapto-*N*-(thiazol-2-yl)acetamide analogs (3a-3h) compounds are shown in Figure 2.

The calculated total energy values for the synthesized molecules obey the following order: 3g < 3e < 3h < 3f < 3c < 3a < 3d < 3b. The final molecules with lower total energy rate indicated that they have a more stable structure, according to computed values of total energy of molecular structures.

The dipole moment of a molecule is a measure of the polarity of the molecule. The value of the dipole moment was also calculated at the DFT/B3LYP/6-

31G(d,p) level using Eqs. (1) and the results are shown in Table 2. Molecule 3f's dipole moment indicates that it is relatively more polarized, while molecule 3c is the less.

In modeling studies where the groups generated from different substituents are used, values of HOMO-LUMO energy, recognized as frontier molecular orbital (FMO) energies, play a pivotal role in determining certain reactivity parameters of the structures.

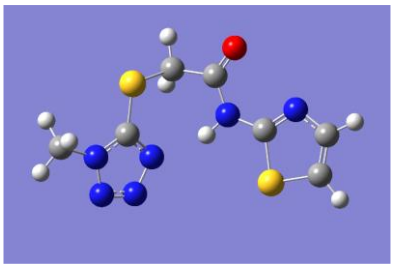

3a

Total Energy: -1471.63175897 a.u.

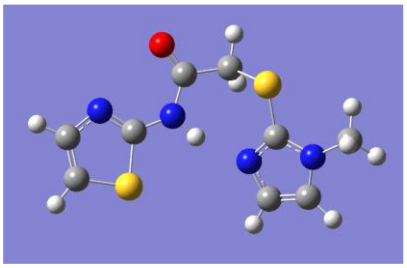

3b

Total Energy: -1439.59825672 a.u.

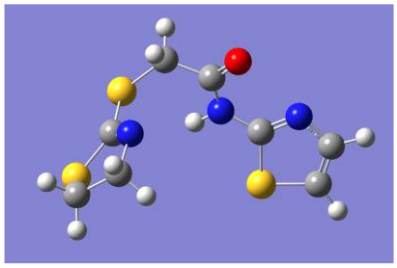

3c

Total Energy: -1744.31660954 a.u.

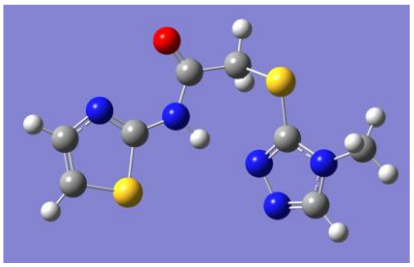

3d

Total Energy: -1455.62007507 a.u.

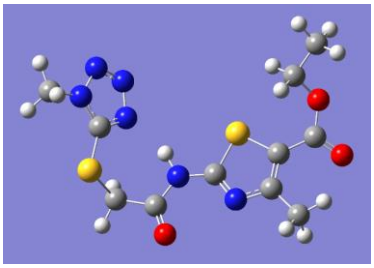

3e

Total Energy: -1778.14166688 a.u.

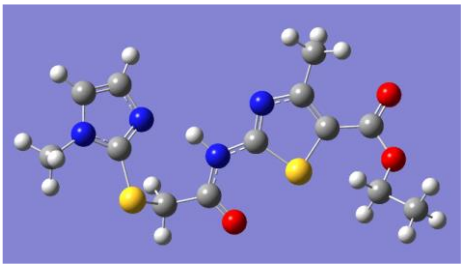

3f

Total Energy: -1746.12065531 a.u.

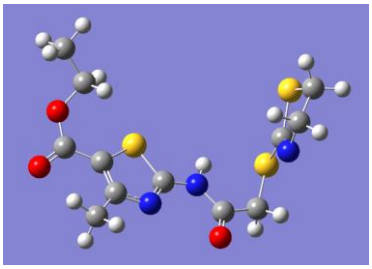

3g

Total Energy: -2050.82615964 a.u.

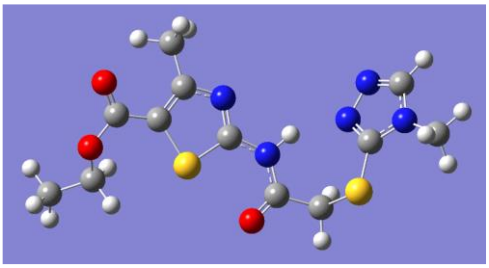

3h

Total Energy: -1762.14140196 a.u.

Figure 2: Optimized molecular structures and total energy values of the compounds **3a-3h** by DFT/B3LYP/6-31G(d,p).

Table 2. The values of electric dipole moment of the compounds 3a-3h.

Compounds	μ_x (Debye)	μ_y (Debye)	μ_z (Debye)	μ_{tot} (Debye)
3a	-4.7926	-0.2548	0.9279	4.8882
3b	-6.4479	-3.8892	0.1782	7.5321
3c	-2.2073	-3.0737	0.6205	3.8347
3d	6.9717	-2.3589	1.1115	7.4434
3e	-8.6135	2.7077	2.4430	9.3537
3f	-9.9239	-1.0354	2.3706	10.2555
3g	5.1377	4.6014	0.6106	6.9240
3h	9.3073	-2.4360	0.5746	9.6379

For the 3a-3h compounds, Table 3 indicates that compound 3e has the smallest energy gap (ΔE) with a value of 0.1664 eV, while compound 3c has the biggest energy gap (E) with a value of 0.1948 eV, indicating that compound 3e is more reactive and so, it's less stable among its analogs.

Table 3. Some reactivity parameters of the compounds 3a-3h.

Compounds	E_{HOMO} (eV)	E_{LUMO} (eV)	ΔE (eV)	I (eV)	A (eV)	χ (eV)	η (eV)	S (eV^{-1})	μ (eV)	ω (eV)
3a	-0.2195	-0.0419	0.1776	0.2195	0.0419	0.1307	0.0888	5.6306	-0.1307	0.0962
3b	-0.2099	-0.0261	0.1838	0.2099	0.0261	0.1180	0.0919	5.4407	-0.1180	0.0758
3c	-0.2259	-0.0311	0.1948	0.2259	0.0311	0.1285	0.0974	5.1335	-0.1285	0.0848
3d	-0.2118	-0.0320	0.1798	0.2118	0.0320	0.1219	0.0899	5.5617	-0.1219	0.0826
3e	-0.2253	-0.0589	0.1664	0.2253	0.0589	0.1421	0.0832	6.0096	-0.1421	0.1213
3f	-0.2164	-0.0481	0.1683	0.2164	0.0481	0.1322	0.0841	5.9453	-0.1322	0.1039
3g	-0.2303	-0.0575	0.1728	0.2303	0.0575	0.1439	0.0864	5.7870	-0.1439	0.1198
3h	-0.2189	-0.0523	0.1666	0.2189	0.0523	0.1356	0.0833	6.0024	-0.1356	0.1104

In Figure 3, HOMO-LUMO orbital diagrams of 3e and 3c compounds were showed, whereas others were showed in Figure S24 (see Supplementary Material).

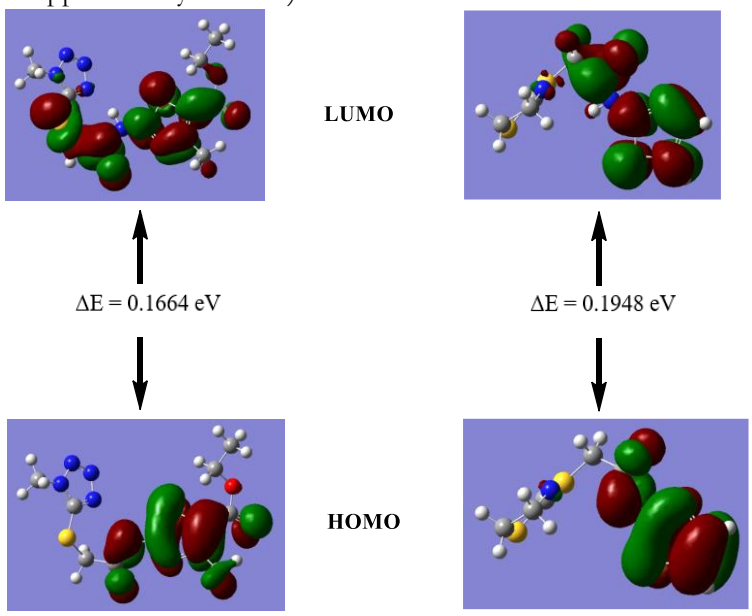

Figure 3: HOMO-LUMO diagrams of the compounds **3e** and **3c** (TD-DFT/B3LYP/6-31G(d,p).

Regarding the compounds in question, 3b exhibits a low ionization potential (I) and a high electron affinity (A) value that are most closely linked to HOMO and LUMO energy.

Target compounds have high χ, in order to 3g > 3e > 3h > 3f > 3a > 3c > 3d > 3b and high ω, in order to 3e > 3g > 3h > 3f > 3a > 3c > 3d > 3b. As seen, compound 3g (0.1439 eV) has a higher electronegativity and 3e (0.1213 eV) has a good electrophilic character than the others. According to the values of chemical hardness-softness (η, S), the compound having the high S and low η value is 3e has been determined.

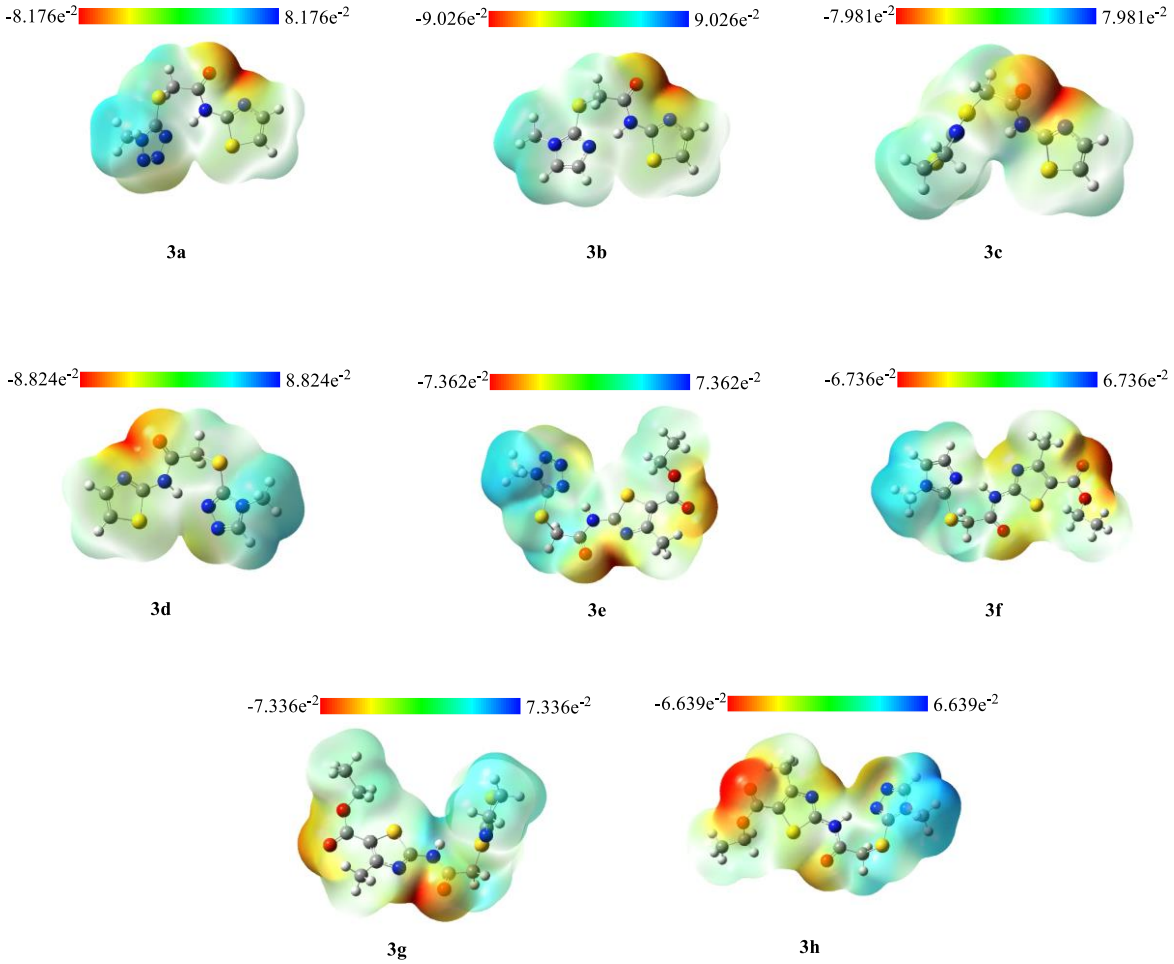

Figure 4: Molecular electrostatic potential (MEP) surfaces presentation of the compounds **3a-3h**

For the 3a–3h compounds, the molecular electrostatic potential (MEP) is shown in Figure 4. According to results, the density functional theory (DFT) calculations on 2-mercapto-*N*-(thiazol-2-yl)acetamide derivatives 3a-3h unveil crucial insights into their stability. The established order, with 3g demonstrating the highest stability, provides a foundation for understanding molecular behavior. This information is pivotal in predicting and rationalizing biological activities of these compounds. Stability is a key determinant in the overall efficacy and safety of drug candidates. The calculated values not only guide the selection of the most stable compounds but also offer valuable cues about potential reactivity. Consequently, DFT becomes an indispensable tool in drug development, aiding in the identification and optimization of compounds with favorable stability profiles that can contribute to enhanced biological activities and therapeutic outcomes.

Biologic activity results

In our study, we first investigated physicochemical properties, then performed a cytotoxic screening on three cancer cell lines and one healthy cell line to be sure that they had potential for further studies. Afterwards, we have achieved very important results.

The cytotoxic properties of the compounds 3a–3h were tested on human-derived A549 non-small cell lung cancer, Caco-2 colorectal cancer, SHSY-5Y neuroblastoma tumor cell lines, and NIH/3T3 mouse fibroblast cell line by using conventional MTT method. IC_{50} values were calculated, and the results were shown in Table 4. Doxorubicin was used as reference drug.

According to results, SHSY-5Y cancer cells were more sensitive than other cancer cells. Mostly, compound 3e has more potential than its analogs in the manner of cancer drug research. A few compounds determined as more active than standard drug, doxorubicin. These are compound 3e (IC_{50}: 46.40±0.43 μg.ml^{-1} and 10.43±0.31 μg.ml^{-1}) against A549 and SHSY-5Y cells, 3c (49.30±0.41 μg.ml^{-1}), 3f (11.87±0.33 μg.ml^{-1})) and 3g (10.74±0.29 μg.ml^{-1}) against SHSY-5Y cells. Overall, compounds did not show cytotoxicity against healthy cells at their IC_{50} values on cancer cells.

Table 4. IC_{50} (μg.ml^{-1}) values of the compounds (3a–3h) against A549, Caco-2, SHSY-5Y tumor and NIH/3T3 fibroblast cell lines

Compounds	A549	Caco-2	SHSY-5Y	NIH/3T3
3a	281.0±0.72	66.60±1.75	63.25±0.39	214.40±0.58
3b	388.80±0.64	284.10±0.76	363.3±0.49	436.30±0.68
3c	89.80±0.91	107.50±0.81	49.30±0.41	>500±0.47
3d	344.0±0.53	328.0±0.64	374.30±0.52	278.50±0.44
3e	46.40±0.43	233.0±0.82	10.43±0.31	291.20±0.64
3f	234.90±0.38	52.10±0.54	11.87±0.33	263.80±0.72
3g	250.20±0.52	205.0±0.77	10.74±0.29	>500±0.37
3h	308.30±0.60	243.0±0.69	71.00±0.48	179.80±0.68
Doxorubicin	86.25±0.25	42.10±0.38	60.20±0.42	202.75±0.29

DISCUSSION

The designed molecules (3a-3h) were synthesized purely with a high yield. The synthesis route is very useful and also cheap; therefore, it can be applied to reproduce the active compounds in a large scale. The drug-likeness of the synthesized compounds is high according to the results of the ADME calculations. With the exception of three compounds (3e, 3g and 3h), gastrointestinal absorption was predicted to be high for probable oral use of the compounds. The activity results indicated that compound 3d is more toxic to healthy cells than three cancer cells. Also, compound 3h is more toxic against healthy cells than A549 lung carcinoma and Caco-2 colorectal adenocarcinoma cells. These findings indicated that the *N*-methyl triazole ring system caused more cytotoxicity effect on NIH/3T3 healthy cells than other azole rings. Furthermore, the thiazoline ring (3c and 3g) had no impact on healthy cells. These two findings suggested together that mercapto azole moiety has a role in selectivity meanwhile aromaticity increases the cytotoxicity in healthy cells which is an unfavorable feature. Analyzing antitumoral activity on A549 cell line, compound 3e exhibited the highest cytotoxicity with selective profile which was better than doxorubicin. Compound 3c was also showed moderate cytotoxicity to same cell line. Meanwhile, in addition to 3d, and 3h, compound 3a is not safe to test for further tests because of high toxicity on healthy cells than A549 cells. Remain compounds (3b, 3f, and 3g) have a narrow IC_{50} range. Results of antitumoral activity on Caco-2 cell line showed that compounds 3a and 3f displayed the highest antiproliferative activity with selectivity. Except 3d and 3h, all compounds affected Caco-2 cells more than healthy cells. However, except for 3a and 3f, the remaining compounds have above 100 μg.ml^{-1} IC_{50} values, so only these two compounds were found valuable in this anti-Caco-2 activity. SHSY-5Y cell line was the most susceptible type against the tested compounds; 3c, 3e, 3f and 3g (IC_{50}: 10.43-49.3 μg.ml^{-1}) showed higher cytotoxicity than the standard drug (IC_{50}: 60.20 μg.ml^{-1}). Besides, compounds 3a and 3h showed remarkable antiproliferative activity. Only compound 3d had more cytotoxicity on SHSY-5Y cells than NIH/3T3 healthy cells; moreover, compounds 3e, 3f, and 3g have very low IC_{50} values (around 10 μg.ml^{-1}). These three compounds have an aryl ethyl carboxylate group, hence, this finding indicated that the ester group has a positive impact and is related to the anti-inflammatory and neuroprotective effects of this group as mentioned previously (Markovic et al. 2023; Osmaniye et al. 2023; Youdim 2013; Yucel et al. 2024). Meanwhile, there was a correlation between anticancer effects against Caco-2 and SHSY-5Y cell lines. It indicated that the anticancer activity on both cell lines of the compounds was affected similarly by the atoms or groups' replacement. On the other hand, it was not observed in this way for the A549 cell line, even most active compound was determined as 3e, compounds 3f and 3g were not effectiveness as much as 3e. So, we suggested that the mechanism of action for compounds against Caco-2 and SHSY-5Y are the same or similar, however, it's different against A549 cells. This difference is probably related to the insulin or ROS sensitivity of both cells as reported (Skora et al. 2022; Szychowski et al. 2019). To clarify this difference, new tests via experimental and computational approaches should be run. Unfortunately, because of the limitation of this study, we can only report potential anticancer agents and the structure-activity relationship in this study.

In summary, SHSY-5Y cells were more sensitive than other cell lines to the final compounds. Additionally, *N*-methyl triazole is not a favorable group since it increased cytotoxicity effect on healthy cells, contrary to the thiazoline ring system.

CONCLUSIONS

In this study, eight *N*-thiazole acetamide analogs were synthesized. Their structural analyses were identified by HRMS, ^{1}H-NMR and ^{13}C-NMR. Their physicochemical properties were calculated using *in silico* methods, and the anticancer activity was evaluated against A549 non-small lung epithelial carcinoma, Caco-2 colon carcinoma, and SHSY-5Y neuroblastoma cells while cytotoxicity effect was

tested against NIH/3T3 fibroblast cells. The results showed that compounds have good ADME profile and chemical stability of the targeted chemicals, compound 3g is the most stable. The predicted physicochemical properties of targeted compounds (3a-3h) indicate compliance with Lipinski's rule of five, suggesting good oral drug potential. Most compounds show high gastrointestinal absorption, with variations in molecular weight, hydrogen bonding, TPSA, and log P values, contributing to their pharmacokinetic profiles. Because it represents the energy balance inside a molecule, stability is important in chemical systems. Final compounds also have significant impact on SHSY-5Y cells with higher selectivity than other cells. Combination of ester group on thiazole and thiazoline (compound 3g) were found significantly effective than doxorubicin and highly selective on SHSY-5Y cells than healthy cells. Besides that, combination of thiazole-triazole (3d and 3h) decreased antiproliferative activity on three cancer cells while increased cytotoxicity on healthy cell. To understand the strength of activity against three cell lines, A549, Caco-2, and SH-SY5Y cell lines, have an important role in clarifying the mechanism of action. Meanwhile, Density Functional Theory (DFT) calculations on targeted compounds (3a–3h) provide critical insights into their stability and reactivity. The total energy values suggest that compound 3g is the most stable, while compound 3e, with the smallest energy gap, is the most reactive. Dipole moment analysis reveals varying polarity, with 3f being the most polarized and 3c the least. Additionally, compound 3e exhibits high chemical softness and low hardness, indicating significant reactivity. The calculated molecular electrostatic potentials further support these findings. These results highlight the utility of DFT in predicting and rationalizing the stability and reactivity of compounds, which are essential for drug development. By identifying the most stable and reactive molecules, DFT aids in the optimization of drug candidates, contributing to improved biological activities and therapeutic outcomes. In particular, insulin-dependent and ROS-related pathways were marked as major possible targets for these compounds. For further studies, these mechanisms will be investigated firstly by computer-aided approaches (CAAs), then experimental studies will be run according to the results from CAA. This study suggests that future perspectives in studies regarding the treatments of neuroblastoma and its related diseases of *ethyl 2-acetamido-4-methylthiazole-5-carboxylate* and thiazoline combination is encouraging.

Conflict of interest: The authors have no conflicts of interest to report.

Authors' Contributions: Conceptualization L.Y., A.E.E.; methodology Z.C., A.E.E., S.D. and D.N.; software A.E.E., S.D. and D.N.; validation L.Y., A.E.E., S.D. and D.N.; formal analysis A.E.E., S.D. and D.N.; investigation A.E.E., S.D., A.Z.K. and D.N.; resources L.Y., A.E.E., Z.C. and D.N.; data curation L.Y., A.E.E., S.D. and D.N.; writing original draft preparation L.Y., A.E.E. and D.N. writing review and editing A.E.E., S.D., A.Z.K., and Z.C.; visualization A.E.E., S.D. and D.N.; supervision L.Y.; project administration A.E.E., and L.Y. All authors have read and agreed to the published version of the manuscript.

Ethical approval: "This study is not subject to the permission of HADYEK in accordance with the "Regulation on Working Procedures and Principles of Animal Experiments Ethics Committees" 8 (k). The data, information and documents presented in this article were obtained within the framework of academic and ethical rules."

Acknowledgement: In this study would like to thank the Anadolu University MERLAB.

REFERENCES

Ahmed, K., Matsuya, Y., Nemoto, H., Zaidi, S.F., Sugiyama, T., Yoshihisa, Y., Shimizu, T., Kondo, T. (2009). Mechanism of apoptosis induced by a newly synthesized derivative of macrosphelides with a thiazole side chain. Chem Biol Interact, 177 (3), 218-226. 10.1016/j.cbi.2008.10.030

Altintop, M.D., Kaplancikli, Z.A., Ciftci, G.A., Demirel, R. (2014). Synthesis and biological evaluation of thiazoline derivatives as new antimicrobial and anticancer agents. Eur. J. Med. Chem., 74, 264-277. 10.1016/j.ejmech.2013.12.060

Bhagat, D.S., Chawla, P.A., Gurnule, W.B., Shejul, S.K., Bumbrah, G.S. (2021). An Insight into Synthesis and Anticancer Potential of Thiazole and 4-thiazolidinone Containing Motifs. Current Organic Chemistry, 25 (7), 819-841. 10.2174/1385272825999210101234704

Bhat, U.G., Halasi, M., Gartel, A.L. (2009). Thiazole antibiotics target FoxM1 and induce apoptosis in human cancer cells. PLoS One, 4 (5), e5592. 10.1371/journal.pone.0005592

Catarzi, D., Varano, F., Vigiani, E., Lambertucci, C., Spinaci, A., Volpini, R., Colotta, V. (2022). Casein Kinase 1delta Inhibitors as Promising Therapeutic Agents for Neurodegenerative Disorders. Curr Med Chem, 29 (27), 4698-4737. 10.2174/0929867329666220301115124

Cavalier, H., Trasande, L., Porta, M. (2023). Exposures to pesticides and risk of cancer: Evaluation of recent epidemiological evidence in humans and paths forward. International Journal of Cancer, 152 (5), 879-912.

Cortes, A.J. (2019). Molecular biology of cancer: similarities between humans and animals. Revista Veterinaria y Zootecnia (On Line), 13 (2), 81-95.

Dawbaa, S., Evren, A.E., Cantürk, Z., Yurttaş, L. (2021). Synthesis of new thiazole derivatives and evaluation of their antimicrobial and cytotoxic activities. Phosphorus Sulfur Silicon Relat Elem, 196 (12), 1093-1102. 10.1080/10426507.2021.1972299

Dawbaa, S., Nuha, D., Evren, A.E., Cankiliç, M.Y., Yurttaş, L., Turan, G. (2023). New oxadiazole/triazole derivatives with antimicrobial and antioxidant properties. J Mol Struct, 1282, 135213. 10.1016/j.molstruc.2023.135213

Delaney, G., Jacob, S., Featherstone, C., Barton, M. (2005). The role of radiotherapy in cancer treatment: estimating optimal utilization from a review of evidence-based clinical guidelines. Cancer, 104 (6), 1129-1137. 10.1002/cncr.21324

Dennington, R., Keith, T., Millam, J. (2009): GaussView, version 5.

Dileep, K., Katiki, M.R., Rao, B.R., Vardhan, V.P.S.V., Sistla, R., Nanubolu, B., Murty, M.S.R. (2017). Regioselective synthesis and preliminary cytotoxic activity properties of tetrazole appendage N-substituted piperazine derivatives. Organic Communications, 10 (3), 178-189. 10.25135/acg.oc.20.17.04.018

Dora, D., Bokhari, S.M.Z., Aloss, K., Takacs, P., Desnoix, J.Z., Szklenarik, G., Hurley, P.D., Lohinai, Z. (2023). Implication of the Gut Microbiome and Microbial-Derived Metabolites in Immune-Related Adverse Events: Emergence of Novel Biomarkers for Cancer Immunotherapy. Int J Mol Sci, 24 (3)10.3390/ijms24032769

El-Gazzar, Y.I., Georgey, H.H., El-Messery, S.M., Ewida, H.A., Hassan, G.S., Raafat, M.M., Ewida, M.A., El-Subbagh, H.I. (2017). Synthesis, biological evaluation and molecular modeling study of new (1,2,4-triazole or 1,3,4-thiadiazole)-methylthio-derivatives of quinazolin-4(3H)-one as DHFR inhibitors. Bioorg Chem, 72, 282-292. 10.1016/j.bioorg.2017.04.019

Eslami, M., Memarsadeghi, O., Davarpanah, A., Arti, A., Nayernia, K., Behnam, B. (2024). Overcoming Chemotherapy Resistance in Metastatic Cancer: A Comprehensive Review. Biomedicines, 12 (1), 183. 10.3390/biomedicines12010183

Evren, A.E., Nuha, D., Dawbaa, S., Karaduman, A.B., Saglik, B.N., Yurttas, L. (2023). Novel oxadiazole-thiadiazole derivatives: synthesis, biological evaluation, and in silico studies. J Biomol Struct Dyn, 1-13. 10.1080/07391102.2023.2247087

Evren, A.E., Yurttas, L., Ekselli, B., Akalin-Ciftci, G. (2019a). Synthesis and biological evaluation of 5-methyl-4-phenyl thiazole derivatives as anticancer agents. Phosphorus Sulfur Silicon Relat Elem, 194 (8), 820-828. 10.1080/10426507.2018.1550642

Evren, A.E., Yurttaş, L., Eksellı, B., Akalın-Cıftcı, G. (2019b). Novel Tri-substituted Thiazoles Bearing Piperazine Ring: Synthesis and Evaluation of their Anticancer Activity. Lett Drug Des Discov, 16 (5), 547-555. 10.2174/1570180815666180731122118

Falzone, L., Bordonaro, R., Libra, M. (2023). SnapShot: Cancer chemotherapy. Cell, 186 (8), 1816-1816.e1811. 10.1016/j.cell.2023.02.038

Freitas, S.C., Sanderson, D., Caspani, S., Magalhaes, R., Cortes-Llanos, B., Granja, A., Reis, S., Belo, J.H., Azevedo, J., Gomez-Gaviro, M.V., Sousa, C.T. (2023). New Frontiers in Colorectal Cancer Treatment Combining Nanotechnology with Photo- and Radiotherapy. Cancers (Basel), 15 (2)10.3390/cancers15020383

Frisch, M., Trucks, G., Schlegel, H., Scuseria, G., Robb, M., Cheeseman, J., Scalmani, G., Barone, V., Mennucci, B., Petersson, G. (2009): Gaussian09, Revision A. Wallingford CT Inc., pp. 150-166.

Gallego, J., Varani, G. (2001). Targeting RNA with small-molecule drugs: therapeutic promise and chemical challenges. Acc Chem Res, 34 (10), 836-843. 10.1021/ar000118k

Hernandes, E.P., Lazarin-Bidoia, D., Bini, R.D., Nakamura, C.V., Cotica, L.F., de Oliveira Silva Lautenschlager, S. (2023). Doxorubicin-Loaded Iron Oxide Nanoparticles Induce Oxidative Stress and Cell Cycle Arrest in Breast Cancer Cells. Antioxidants (Basel), 12 (2)10.3390/antiox12020237

Hernández-Paredes, J., Glossman-Mitnik, D., Duarte-Moller, A., Flores-Holguín, N. (2009). Theoretical calculations of molecular dipole moment, polarizability, and first hyperpolarizability of glycine–sodium nitrate. Journal of Molecular Structure: THEOCHEM, 905 (1-3), 76-80. 10.1016/j.theochem.2009.03.014

Hoelder, S., Clarke, P.A., Workman, P. (2012). Discovery of small molecule cancer drugs: successes, challenges and opportunities. Mol Oncol, 6 (2), 155-176. 10.1016/j.molonc.2012.02.004

Holohan, C., Van Schaeybroeck, S., Longley, D.B., Johnston, P.G. (2013). Cancer drug resistance: an evolving paradigm. Nat Rev Cancer, 13 (10), 714-726. 10.1038/nrc3599

Housman, G., Byler, S., Heerboth, S., Lapinska, K., Longacre, M., Snyder, N., Sarkar, S. (2014). Drug resistance in cancer: an overview. Cancers (Basel), 6 (3), 1769-1792. 10.3390/cancers6031769

Kavitha, J., Sivakrishnan, S., Srinivasan, N. (2022). Self-Medication in Today's Generation without Knowledge as Self Inflicted Harm. Archives Of Pharmacy Practice, 13 (3), 16-22. 10.51847/PXyGs4x42h

Kleinman, D.A. (1962). Nonlinear Dielectric Polarization in Optical Media. Physical Review, 126 (6), 1977-1979. 10.1103/PhysRev.126.1977

Kwon, J.H., Tanco, K., Park, J.C., Wong, A., Seo, L., Liu, D., Chisholm, G., Williams, J., Hui, D., Bruera, E. (2015). Frequency, Predictors, and Medical Record Documentation of Chemical Coping Among Advanced Cancer Patients. Oncologist, 20 (6), 692-697. 10.1634/theoncologist.2015-0012

Laiolo, J., Graikioti, D.G., Barbieri, C.L., Joray, M.B., Antoniou, A.I., Vera, D.M.A., Athanassopoulos, C.M., Carpinella, M.C. (2024). Novel betulin derivatives as multidrug reversal agents targeting P-glycoprotein. Sci Rep, 14 (1), 70. 10.1038/s41598-023-49939-9

Li, Q., Xu, N., Lin, M., Chen, Y., Li, H. (2024). Successful treatment of severe lung cancer caused by third-generation EGFR-TKI resistance due to EGFR genotype conversion with afatinib plus anlotinib. Anticancer Drugs, 35 (1), 93-96. 10.1097/CAD.0000000000001530

Markovic, A., Zivkovic, A., Atanasova, M., Doytchinova, I., Hofmann, B., George, S., Kretschmer, S., Rodl, C., Steinhilber, D., Stark, H., Smelcerovic, A. (2023). Thiazole derivatives as dual inhibitors of deoxyribonuclease I and 5-lipoxygenase: A promising scaffold for the development of neuroprotective drugs. Chem Biol Interact, 381, 110542. 10.1016/j.cbi.2023.110542

McGhee, W.R., Dempster, M., Graham-Wisener, L. (2022). The role of companion animals in advanced cancer: an interpretative phenomenological analysis. BMC palliative care, 21 (1), 160.

Nitkin, P. (2014): Being there: relationships between people with cancer and their pets: what helps and what hinders. University of British Columbia.

Nitkin, P., Buchanan, M.J. (2020). Relationships between people with cancer and their companion animals: what helps and hinders. Anthrozoös, 33 (2), 243-259.

Nuha, D., Evren, A.E., Ciyanci, Z.S., Temel, H.E., Akalin Ciftci, G., Yurttas, L. (2022). Synthesis, density functional theory calculation, molecular docking studies, and evaluation of novel 5-nitrothiophene derivatives for anticancer activity. Arch Pharm (Weinheim), 355 (9), e2200105. 10.1002/ardp.202200105

Nuha, D., Evren, A.E., Kapusiz, Ö., Gül, Ü.D., Gundogdu-Karaburun, N., Karaburun, A.Ç., Berber, H. (2023).

Design, synthesis, and antimicrobial activity of novel coumarin derivatives: An in-silico and in-vitro study. J Mol Struct, 1272, 134166. 10.1016/j.molstruc.2022.134166

Ocansey, D.K.W., Qian, F., Cai, P., Ocansey, S., Amoah, S., Qian, Y., Mao, F. (2024). Current evidence and therapeutic implication of PANoptosis in cancer. Theranostics, 14 (2), 640-661. 10.7150/thno.91814

Oh, J.H., Cho, J.-Y. (2023a). Comparative oncology: overcoming human cancer through companion animal studies. Experimental & Molecular Medicine, 55 (4), 725-734.

Oh, J.H., Cho, J.Y. (2023b). Comparative oncology: overcoming human cancer through companion animal studies. Exp Mol Med, 55 (4), 725-734. 10.1038/s12276-023-00977-3

Osmaniye, D., Evren, A.E., Karaca, Ş., Özkay, Y., Kaplancıklı, Z.A. (2023). Novel thiadiazol derivatives; design, synthesis, biological activity, molecular docking and molecular dynamics. J Mol Struct, 1272, 134171. 10.1016/j.molstruc.2022.134171

Osmaniye, D., Levent, S., Sağlık, B.N., Karaduman, A.B., Özkay, Y., Kaplancıklı, Z.A. (2022). Novel imidazole derivatives as potential aromatase and monoamine oxidase-B inhibitors against breast cancer. New Journal of Chemistry, 46 (16), 7442-7451. 10.1039/d2nj00424k

Özkay, Y., Evren, A.E., Yurttaş, L. (2022). Synthesis and In Silico Evaluation of Some New 2,4-Disubstituted Thiazole Derivatives. European Journal of Life Sciences, 1 (1), 8-19. 10.55971/ejls.1089425

Pinho, S.S., Carvalho, S., Cabral, J., Reis, C.A., Gartner, F. (2012). Canine tumors: a spontaneous animal model of human carcinogenesis. Transl Res, 159 (3), 165-172. 10.1016/j.trsl.2011.11.005

Roskoski Jr, R. (2024). Properties of FDA-approved small molecule protein kinase inhibitors: a 2024 update. Pharmacological research, 107059.

Saffour, S., Al-Sharabi, A.A., Evren, A.E., Cankiliç, M.Y., Yurttaş, L. (2024). Antimicrobial activity of novel substituted 1,2,4-triazole and 1,3-thiazole derivatives. J Mol Struct, 1295, 136675. 10.1016/j.molstruc.2023.136675

Sarver, A.L., Makielski, K.M., DePauw, T.A., Schulte, A.J., Modiano, J.F. (2022). Increased risk of cancer in dogs and humans: A consequence of recent extension of lifespan beyond evolutionarily determined limitations? Aging and cancer, 3 (1), 3-19.

Sharifi, M., Hosseinali, S.H., Saboury, A.A., Szegezdi, E., Falahati, M. (2019). Involvement of planned cell death of necroptosis in cancer treatment by nanomaterials: Recent advances and future perspectives. J Control Release, 299, 121-137. 10.1016/j.jconrel.2019.02.007

Singh, A., Malhotra, D., Singh, K., Chadha, R., Bedi, P.M.S. (2022). Thiazole derivatives in medicinal chemistry: Recent advancements in synthetic strategies, structure activity relationship and pharmacological outcomes. J Mol Struct, 133479. 10.1016/j.molstruc.2022.133479

Skora, B., Lewinska, A., Kryshchyshyn-Dylevych, A., Kaminskyy, D., Lesyk, R., Szychowski, K.A. (2022). Evaluation of Anticancer and Antibacterial Activity of Four 4-Thiazolidinone-Based Derivatives. Molecules, 27 (3)10.3390/molecules27030894

Szychowski, K.A., Kaminskyy, D.V., Leja, M.L., Kryshchyshyn, A.P., Lesyk, R.B., Tobiasz, J., Wnuk, M., Pomianek, T., Gminski, J. (2019). Anticancer properties of 5Z-(4-fluorobenzylidene)-2-(4-hydroxyphenylamino)-thiazol-4-one. Sci Rep, 9 (1), 10609. 10.1038/s41598-019-47177-6

Tarighati, E., Keivan, H., Mahani, H. (2023). A review of prognostic and predictive biomarkers in breast cancer. Clin Exp Med, 23 (1), 1-16. 10.1007/s10238-021-00781-1

Tolomeo, M., Simoni, D. (2002). Drug resistance and apoptosis in cancer treatment: development of new apoptosis-inducing agents active in drug resistant malignancies. Curr Med Chem Anticancer Agents, 2 (3), 387-401. 10.2174/1568011024606361

Wang, Y.-T., Huang, X., Cai, X.-C., Kang, X.-X., Zhu, H.-L. (2024). Synthesis, biological evaluation and molecular docking of thiazole hydrazone derivatives grafted with indole as novel tubulin polymerization inhibitors. J Mol Struct, 1301, 137343. 10.1016/j.molstruc.2023.137343

Wu, P., Nielsen, T.E., Clausen, M.H. (2015). FDA-approved small-molecule kinase inhibitors. Trends Pharmacol Sci, 36 (7), 422-439. 10.1016/j.tips.2015.04.005

Xing, X., Pang, E., Zhao, S., Pan, T., Tan, Q., Wang, B., Song, X., Lan, M. (2024). Cisplatin-appended BODIPY for near infrared II fluorescent and photoacoustic imaging-guided synergistic phototherapy and chemotherapy of cancer. Chinese Chemical Letters, 35 (3), 108467. 10.1016/j.cclet.2023.108467

Xiong, B., Chen, S., Zhu, P., Huang, M., Gao, W., Zhu, R., Qian, J., Peng, Y., Zhang, Y., Dai, H., Ling, Y. (2019). Design, Synthesis, and Biological Evaluation of Novel Thiazolyl Substituted Bis-pyrazole Oxime Derivatives with Potent Antitumor Activities by Selectively Inducing Apoptosis and ROS in Cancer Cells. Med Chem, 15 (7), 743-754. 10.2174/1573406414666180827112724

Xiong, L., Zhang, Y., Wang, J., Yu, M., Huang, L., Hou, Y., Li, G., Wang, L., Li, Y. (2024). Novel small molecule inhibitors targeting renal cell carcinoma: Status, challenges, future directions. Eur J Med Chem, 116158.

Yang, C.Y., Shiranthika, C., Wang, C.Y., Chen, K.W., Sumathipala, S. (2023). Reinforcement learning strategies in cancer chemotherapy treatments: A review. Comput Methods Programs Biomed, 229, 107280. 10.1016/j.cmpb.2022.107280

Youdim, M.B. (2013). Multi target neuroprotective and neurorestorative anti-Parkinson and anti-Alzheimer drugs ladostigil and m30 derived from rasagiline. Exp Neurobiol, 22 (1), 1-10. 10.5607/en.2013.22.1.1

Yucel, N.T., Asfour, A.A.R., Evren, A.E., Yazici, C., Kandemir, U., Ozkay, U.D., Can, O.D., Yurttas, L. (2024). Design and synthesis of novel dithiazole carboxylic acid Derivatives: In vivo and in silico investigation of their Anti-Inflammatory and analgesic effects. Bioorg Chem, 144, 107120. 10.1016/j.bioorg.2024.107120

Yurttas, L., Evren, A.E., AlChaib, H., Temel, H.E., Akalin Ciftci, G. (2024). Synthesis, molecular docking, and molecular dynamic simulation studies of new 1,3,4-thiadiazole derivatives as potential apoptosis inducers in A549 lung cancer cell line. J Biomol Struct Dyn, 1-16. 10.1080/07391102.2023.2300125

Yurttaş, L., Çavuşoğlu, B.K., Cantürk, Z. (2020). Novel 2-(2-hydrazinyl)thiazole derivatives as chemotherapeutic agents. Synth. Commun., 50 (20), 3072-3079. 10.1080/00397911.2020.1791344

Yurttaş, L., Evren, A.E., Kubilay, A., Aksoy, M.O., Temel, H.E., Akalın Çiftçi, G. (2023). Synthesis of Some New 1,3,4-Oxadiazole Derivatives and Evaluation of Their Anticancer Activity. ACS Omega, 10.1021/acsomega.3c07776

Yurttaş, L., Öztürk, Ö., Cantürk, Z. (2019). New Procaspase Activating Compound (PAC-1) Like Molecules as Potent Antitumoral Agents Against Lung Cancer. Lett Drug Des Discov, 16 (6), 645-655. 10.2174/1570180815666180926113040